Atmospheric Environment 366 (2026) 121666

Contents lists available at ScienceDirect

Atmospheric Environment

journal homepage: www.elsevier.com/locate/atmosenv

Revealing long-term anthropogenic influence on PM_{10} through lead isotope signatures in a post-mining region

Tjaša Žerdoner [a,b], Judita Burger [c], Irena Kranjc [c], Janja Turšič [c], Tea Zuliani [a,b,*]

[a] Jožef Stefan International Postgraduate School, Jamova 39, Ljubljana, Slovenia
[b] Jožef Stefan Institute, Department of Environmental Sciences, Jamova 39, Ljubljana, Slovenia
[c] Slovenian Environment Agency, Vojkova cesta 1 b, Ljubljana, Slovenia

HIGHLIGHTS

- Investigation of PM_{10} sources using elemental and Pb isotope data.
- Temporal variations in PTEs concentrations and Pb isotopes observed.
- Anthropogenic Pb contributed 55.8 %–69.3 % to PM_{10} highlighting human activity impact.
- Study highlights the need to address historical and current sources of Pb pollution.

GRAPHICAL ABSTRACT

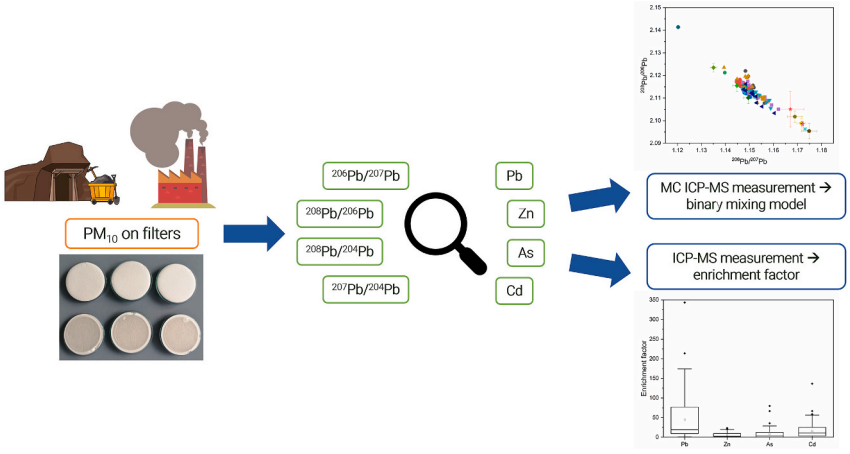

ARTICLE INFO

Keywords:
Source apportionment
Pb isotopes
PTEs
MC ICP-MS
Upper Meža Valley

ABSTRACT

This study investigated long-term anthropogenic contributions to airborne particulate matter (PM_{10}) in the Upper Meža Valley, Slovenia, a region historically affected by ore mining, smelting, and, more recently, secondary Pb production. PM_{10} samples collected at five locations in the summer and autumn of 2018 and at one location in the spring and summer of 2021 were analysed for elemental composition and Pb isotope ratios to identify and quantify pollution sources. Elevated concentrations of Pb, Zn, Cd, and As were observed across all sites, with minimal temporal variations. Enrichment factor (EF) analysis indicated lower EF values for Zn and As, suggesting a primarily crustal origin. Conversely, higher EF values for Cd and Pb pointed to mixed crustal and anthropogenic sources. The proportion of PM_{10} samples with high Pb enrichment increased from 9.09 % in 2018 to 20.5 % in 2021, indicating a rising influence of anthropogenic emissions. This study represents the first application of Pb isotope composition and a two-endmember mixing model for detailed source apportionment of PM_{10} in the region. The Pb isotope ratios of PM_{10} samples fell between local geogenic background and known anthropogenic sources, with anthropogenic contributions accounting for 55.8 %–69.3 % of total Pb in PM_{10}.

* Corresponding author. Jožef Stefan Institute, Department of Environmental Sciences, Jamova 39, Ljubljana, Slovenia.
E-mail address: tea.zuliani@ijs.si (T. Zuliani).

https://doi.org/10.1016/j.atmosenv.2025.121666
Received 18 June 2025; Received in revised form 25 October 2025; Accepted 8 November 2025
Available online 10 November 2025

These findings have important implications for local environmental management, as they can support targeted mitigation strategies, which are critical for public health protection.

1. Introduction

Airborne particulate matter PM_{10} refers to particles, solid and/or liquid droplets suspended in air, with a diameter of 10 μm or less, which can originate from various natural and anthropogenic sources (European Environment Agency Glossary, 2025). Chemically, PM_{10} can be made of a single component or may comprise a mix of substances such as elements, sulphates, nitrates, ammonia, sodium chloride, carbon, mineral dust, and microorganisms (Faraji et al., 2019). PM_{10} particles are small enough to be inhaled into the respiratory system, causing or exacerbating respiratory diseases such as asthma, bronchitis, and other lung conditions (Nikoonahad et al., 2017). Prolonged exposure to high levels of PM_{10} has also been linked to cardiovascular issues and can significantly affect vulnerable populations, including children, the elderly, and those with pre-existing health conditions (Bodor et al., 2021). These effects on human health are strongly correlated with the residence time of particulate matter in the air. The residence time is largely determined by particle size and atmospheric conditions, for PM_{10} being reported between 10 and 12 h (Di Girolamo, 2020; Vecchi et al., 2007).

Mineral PM_{10} particles are of particular concern due to their potential to contain potentially toxic elements (PTEs), like lead (Pb), zinc (Zn), cadmium (Cd), and arsenic (As), among others (Manalis et al., 2005). The presence of these elements in PM_{10} poses an additional hazard, as inhalation can lead to PTEs accumulation in the human body, posing severe health risks. Pb exposure can cause neurological and developmental issues, especially in children (Ettler, 2016; Needleman, 2004); Cd is known for its carcinogenic properties; As exposure can lead to skin lesions and has been linked to various cancers; and high levels of Zn can disrupt bodily functions (Csavina et al., 2012; Entwistle et al., 2019). These particles can originate from natural sources like soil and rock dust or anthropogenic activities such as mining, recycling of waste materials (mine waste, batteries, …), and construction. Therefore, understanding the composition of mineral PM_{10} particles and their origin helps mitigate their presence in the air and is critical for ensuring public health safety.

PM_{10} can be transported over long distances through atmospheric, hydrological, and food pathways, making it difficult to determine their sources. Numerous researchers have tried to identify the various sources and pathways of PTEs contamination by analysing concentration variances and enrichment factors compared to natural background levels (Beane et al., 2016; Doufexi et al., 2022; Yoshinaga et al., 2014). However, monitoring only PTEs concentrations at different locations and sample types, and knowing from which activities they may be released into the environment, is often not enough to determine their origin in the PM_{10} and the contributions of individual sources to the overall pollution. In recent years, the stable isotope composition of different elements has been used. This is made possible by significant advancements in the precision of mass spectrometers, which can now detect subtle differences in isotope compositions. One element whose isotope composition can offer valuable insights into its origin within a sample is Pb (Dewan et al., 2015; Dong et al., 2017; Félix et al., 2015). The isotope composition of Pb is not significantly affected by physicochemical processes, therefore, it provides an efficient tool for determining sources and pathways of Pb (Bollhöfer and Rosman, 2001; Shiel et al., 2010). The isotope ratios of Pb in a mineral are influenced by the original amount of Pb isotopes and parent isotopes in the material, and the duration for which Pb and its parent isotopes remained together before Pb was incorporated into the mineral. In environmental contexts, Pb isotope ratios illustrate the blending of naturally occurring sources with human-derived ones. These mixing processes can be quantified, provided that each Pb source possesses a unique isotopic signature (Kong et al., 2018; Li et al., 2012, 2018). A challenge in using Pb isotopes as source tracers occurs when the Pb isotope compositions of potential source end-members (terrestrial or anthropogenic) are not well-defined, overlap, or when the anthropogenic Pb originates from multiple sources over time (Sen et al., 2016).

In the Upper Meža Valley lies the largest Pb and Zn ore deposit in Slovenia, with a long history of mining and smelting. During the mine's lifespan, 19 million tons of Pb and Zn ore were excavated, from which 1 million tons of Pb and 0.5 million tons of Zn were extracted (Rečnik et al., 2014). During processing, a large amount of mine waste containing high concentrations of Pb, Zn, As, Cd, and other PTEs, was produced and deposited in abandoned mine shafts and near the small streams along the Upper Meža Valley (Žibret et al., 2018). As a result, the Upper Meža Valley was excessively polluted with Pb, Zn, and other PTEs (Finzgar et al., 2014; Goltnik et al., 2022; Gošar et al., 2015; Gosar and Miler, 2011). Residents were daily exposed to these elements through dust, mainly by inhalation and/or ingestion. Elevated PTEs levels, particularly Pb, were observed in the Upper Meža Valley population, with young children most at risk. Blood testing for Pb began in 1974, when preschool children had median levels above 400 μg/L (Jez and Lestan, 2015). By 1990, the concentrations decreased to 41–284 μg/L. In 2001–2002, over one-third of children still had elevated Pb levels (>100 μg/L), decreasing to one-fifth of 3-year-olds in 2017 (Snoj Tratnik et al., 2019). Pb monitoring in PM_{10} in Žerjav, formerly a Pb smelter site, has continued since 1972 (Fig. S1, Supplementary). Although Pb concentrations in PM_{10} decreased sharply from 1972 to 2007, annual averages rose again from 250 ng/m^3 to 700 ng/m^3 between 2010 and 2021 (Ivartnik et al., 2019, 2022).

The Upper Meža Valley is located within the geologically complex Karavanke Mountain Range, an area of significant mineralisation formed during the Alpidic orogenesis. The region hosts world-class Pb-Zn ore deposits, including the Mežica deposit in the Middle and Upper Triassic Wetterstein and Partnach strata, and the unique Topla Zn-Pb stratiform deposit in Mt. Peca. Rich depositions of ores and minerals underscore the valley's important geological and mining heritage, making it a critical site for studying natural and anthropogenic Pb sources. Previous research in the Upper Meža Valley has primarily focused on assessing the distribution and environmental burden of PTEs, whereas detailed isotopic source apportionment of Pb and quantification of individual source contributions have not yet been comprehensively investigated. The only previous indication that secondary Pb production activities may influence atmospheric Pb levels in the valley was reported by Miler and Gosar (2013) (Miler and Gosar, 2013), who identified Pb-bearing particles in snow using SEM-EDS analysis, without isotopic confirmation (Miler and Gosar, 2013). In contrast, the present study provides the first systematic investigation combining Pb isotope ratios with PTEs concentrations in airborne particulate matter (PM_{10} and $PM_{2.5}$) and related environmental media in the Upper Meža Valley. For the first time, an extensive and region-specific database of Pb isotope ratios and PTEs concentrations has been established for PM_{10}, $PM_{2.5}$, soil, sand, mine waste, river sediment, ores, and locally produced battery components. Based on this dataset, a Pb isotopic mixing model was applied to identify and quantify contributions from natural geological sources and secondary anthropogenic emissions. This integrated isotopic and geochemical approach provides novel insights into Pb source dynamics and atmospheric contamination processes in one of Slovenia's most historically polluted mining regions.

2. Materials and methods

2.1. Sampling and sample preparation

The Upper Meža Valley is a narrow valley at 480 m above sea level, situated between steep hills in NE Slovenia. PM_{10} samples were collected in August, September and October of 2018, at five different sampling locations (#1 – #5) in the Upper Meža Valley, in the settlements of Žerjav and Črna na Koroškem (Fig. 1). More information about sampling locations is provided in the Supplementary. An additional sampling was performed in Žerjav in March, April, May, June and August of 2021 at Location #1 (Fig. 1). At Location #1, a regular PM_{10} monitoring station from the National Environment Agency (ARSO) is situated. The number of samples collected each month at each location is shown in Table S1 (Supplementary). Samples were not collected throughout the whole year, they were primarily collected in summer and fall to compare the working and vacation days. In addition to PM_{10}, $PM_{2.5}$ samples were also collected in 2018 at Location #4.

Sampling of PM_{10} at Locations #1, #2, #3, #5, and of $PM_{2.5}$ at Location #4 was performed with a reference low-volume sequential sampler Leckel SEQ 47/50, with pre-annealed 47 mm quartz fibre filters (MN QF-10, 47 mm, Macherey-Nagel, Düren, Germany). The filters were automatically changed every 24 h at a predetermined time. The airflow through the filter was 55.2 m^3/day. On the other hand, sampling of PM_{10} at Location #4 was performed with a high-volume DIGITEL DHA-80 sampler, with 150 mm quartz fibre filters. The filters were automatically changed every 24 h at a predetermined time. The airflow through the filter was 720 m^3/day.

In addition to PM_{10}, other types of samples, considered as potential sources of PTEs in PM_{10}, were also collected and analysed, such as local soil, sand, sediment, mine waste, and exhaust from the secondary Pb production industry. As an approximation of emissions from secondary Pb production, namely Pb-battery production industry, components of Pb-batteries produced in the area were analysed. For the purpose of this study, soil, sand, sediment and mine waste samples were considered as local background, and exhausts from the Pb-battery production industry were considered as an anthropogenic source. Soil, sand, and mine waste samples were obtained from ARSO. Sediment samples were collected in January 2020, and details concerning their collection from the Meža River and its tributaries are provided in the article by Goltnik et al. (2022) (Goltnik et al., 2022).

2.2. Instrumentation

Filters with PM_{10} were digested with the closed vessel microwave digestion system (UltraWAVE, Milestone, Sorisole, BG, Italy). Samples of sediment, soil, sand, mine waste and ore were digested with the closed vessel microwave digestion system (MARS 6, CEM Corporation, Matthews, NC, USA). Samples of battery components (Pb-grid and Pb-paste composed of PbO and $PbSO_4$) were digested on a hotplate (C-MAG HP 10, IKA-Werke, Staufen, Germany). Total elemental concentrations were determined by quadrupole-ICP-MS (7700x, Agilent Technologies, Tokyo, Japan). ICP-MS operating parameters were optimised daily for the highest sensitivity and are presented in Table S2 (Supplementary). The Pb isotope ratios were determined by a Nu II Plasma MC ICP-MS from Nu Instruments (Ametek, Berwyn, MD, USA) coupled to a desolvation system (Aridus from Teledyne Cetac, Omaha, NE, USA) with a PFA nebulizer (100 μL/min) and nickel plasma cones for dry plasma. The instrument was optimised daily for the highest sensitivity and stability of the signal. General parameters are presented in Table S2 (Supplementary).

2.3. Reagents and materials

For the preparation of samples and reagents, Ultrapure 18.2 MΩ cm water obtained from a Direct Q 5 system (Millipore, Watertown, MA,

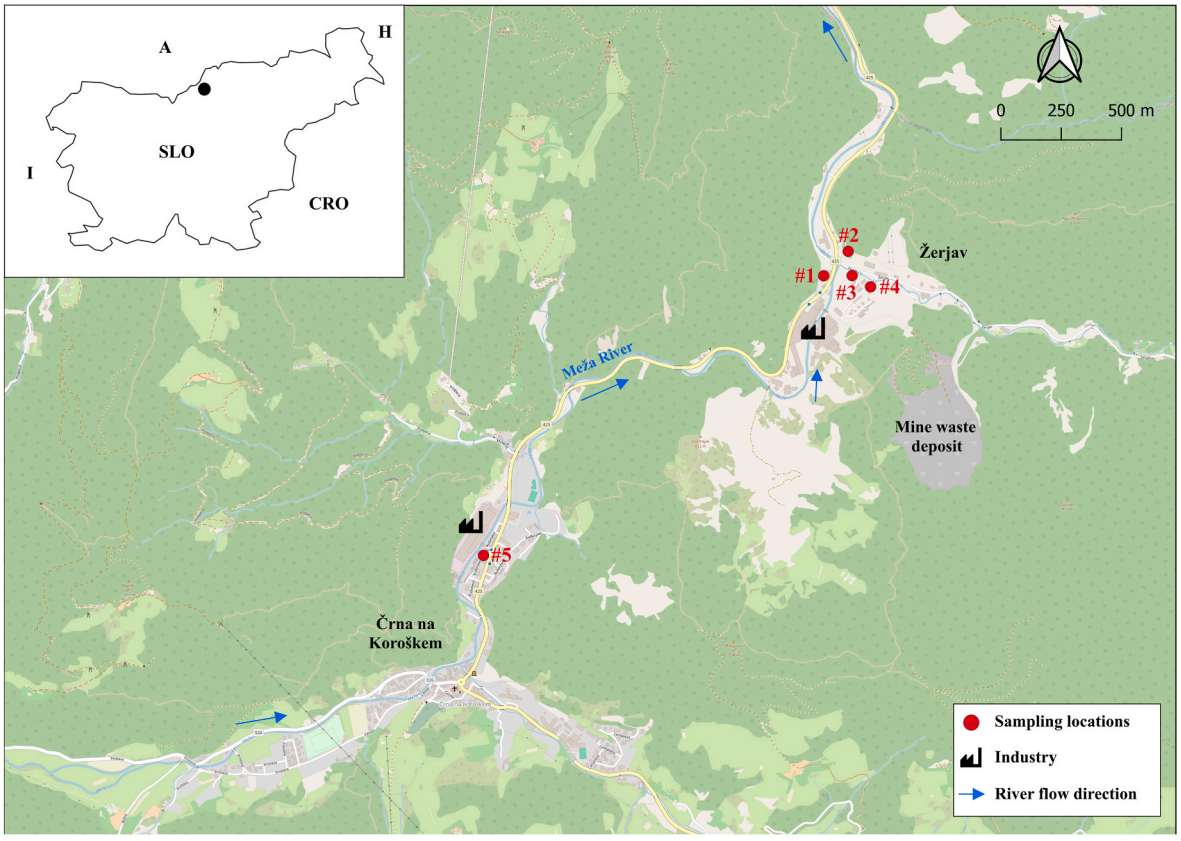

Fig. 1. Sampling area with sampling locations.

USA) was used. Hydrochloric acid (30 % (*w/w*) HCl, suprapur) and hydrofluoric acid (40 % (*w/w*) HF, suprapur) were obtained from Merck Ltd. (Darmstadt, Germany). Nitric acid (67–69 % (*w/w*) HNO_3, suprapur) was obtained from Carlo Erba Reagents Srl (Milan, Italy). Hydrogen peroxide (30 % (*w/w*) H_2O_2, suprapur) and boric acid (H_3BO_3, ultrapur) were obtained from Sigma-Aldrich (St. Louis, MO, USA). For the determination of total elemental concentrations, an external calibration was used, prepared with the dilution of a multielement standard solution, Multi VI (ICP Standard Certipur, Merck, Darmstadt, Germany). As an accuracy check, certified reference materials of PM_{10}-like fine dust ERM-CZ120 (Institute for Reference Materials and Measurements, Geel, Belgium), channel sediment BCR 320R (Institute for Reference Materials and Measurements, Geel, Belgium), loam soil ERM-CC141 (Institute for Reference Materials and Measurements, Geel, Belgium) and certified reference material for trace elements in surface water SPS-SW1 (Spectrapure standards, Oslo, Norway) were used. The determined values for all materials were in good alignment with the certified values (Table S3 (Supplementary)). For Pb isotope ratio determination, SRM 981, a Pb isotope certified reference material and SRM 3158, a Tl standard solution, both from NIST (National Institute of Standards and Technology, Maryland, USA), were used.

2.4. Analytical procedures

Filters with PM_{10} were digested with a closed vessel microwave-assisted digestion following the standard *EN 14902 Ambient Air Quality. Standard Method for the Measurement of Pb, Cd, As, and Ni in the PM_{10} Fraction of Suspended Particulate Matter* (EN 14902 Ambient air quality, 2005). Filters were put into Teflon vessels, and 8 mL of HNO_3 and 2 mL of H_2O_2 were added. The samples were subjected to one cycle of closed vessel microwave digestion at the maximum power of 1500 W. A clear solution was quantitatively transferred into a 100 mL measuring flask and filled to the mark with MilliQ water. The same procedure (acids only) was applied to a blank sample in every cycle.

Soil, sand, sediment, mine waste, and ore samples were digested with a closed vessel microwave-assisted digestion following the method described by Zuliani et al. (2016) (Zuliani et al., 2016). First, approximately 0.25 g of a sample was weighed into Teflon vessels. Afterwards, 4 mL of HNO_3, 2 mL of H_2O_2, 1 mL of HCl, and 2 mL of HF were added. The samples were subjected to two cycles of closed vessel microwave digestion at the maximum power of 1600 W. After the first cycle, H_3BO_3 (4 % (*w/w*)) was added, and the samples were subjected to the second cycle of microwave digestion. A clear solution was quantitatively transferred into 30 mL PP graduated tubes and filled to the mark with MilliQ water. The same procedure (acids only) was applied to a blank sample in every cycle. As an accuracy check, certified reference materials of PM_{10}-like fine dust ERM-CZ120, channel sediment BCR 320R, and loam soil ERM-CC141 were subjected to the same digestion procedure as samples.

To ensure that results from the two digestion procedures could be compared, some PM_{10} filters were also digested using the soil sample digestion method (which included HF). The concentrations of Pb, Zn, As, Cd, and Fe were comparable between the two digestion procedures. As expected, only Al showed a difference (data not shown). Based on this comparison, Pb, Zn, As, Cd, and Fe concentrations were considered consistent across the different sample types.

Battery components were digested on a hotplate with 8 M HNO_3. Approximately 0.05 g of a sample was weighed into 50 mL PP graduated tubes, and 15 mL of 8 M HNO_3 was added. The closed tubes were put on a hotplate at around 85 °C for 6 h. As an accuracy check, certified reference material NIST SRM 981 Pb isotopic standard was subjected to the same digestion procedure as samples. The digestion efficiency was checked with standard addition – Pb, Zn, As, Cd, and Fe standards were added to the samples in a concentration ratio in sample *vs.* standard as 1 *vs.* 2.

Pb isotope ratio determination in samples was done as described by Goltnik et al. (2022) (Goltnik et al., 2022). Briefly, Pb was isolated from the matrix by using an ion exchange resin Dowex® 1X8 (100–200 mesh, Acros Organics, Geel, Belgium). Pb was washed out of the resin by 6 M HCl. The samples were then evaporated to dryness and redissolved in 6 mL of 2 % HNO_3. To control Pb recovery after separation, the total Pb concentration was measured by ICP-MS. Lead isotope ratios were determined by MC ICP-MS. For the correction of instrumental mass bias, a combination of internal (standard-sample bracketing method) and external (Russell law) corrections was used (Yang et al., 2018). For internal correction, an appropriate amount of standard solution of Tl (NIST SRM 3158) was added to the samples before the measurement (Tl concentration in the sample was 4 times lower than that of Pb). The Pb isotope standard reference material NIST SRM 981 was measured as a bracketing standard. Determined Pb isotope ratios in NIST SRM 981 are presented in Table S4 (Supplementary).

2.5. Calculation of enrichment factor (EF)

The enrichment factor (EF) for Pb, Zn, Cd, and As in PM_{10} samples was used for identifying their possible anthropogenic input. It was calculated using the following equation:

$$EF = \frac{(X/R)_{aerosol}}{(X/R)_{crust}} \quad (1)$$

where X represents the element of interest, R is the reference element, and $(X/R)_{aerosol}$ and $(X/R)_{crust}$ represent the concentration ratios of X and R in PM_{10} samples and the Earth's upper crust, respectively. Different elements can be used as reference elements, the most commonly Si, Al, and Fe, as they are abundant in the crust (Cesari et al., 2012; Enamorado-Báez et al., 2015). In this study, Fe was used as a reference element. For the $(X/Fe)_{crust}$, an average value from all the measured samples of local soil was taken. Based on EF values, sources of elements are categorised into three groups: $EF < 10$ contributions primarily from crustal source; $10 < EF < 100$ contributions from mixed sources, crustal and anthropogenic; and $EF > 100$ contributions primarily from anthropogenic source (Lee et al., 2017).

2.6. Calculation of the binary mixing model of Pb isotope ratios

The relative contribution of a possible anthropogenic source to Pb in PM_{10} was calculated using an equation for the binary mixing model (Monna et al., 1997):

$$Pb_{anthropogenic}\ (\%) = \frac{\left(^{206}pb/^{207}Pb\right)_{sample} - \left(^{206}pb/^{207}Pb\right)_{natural}}{\left(^{206}pb/^{207}Pb\right)_{anthropogenic} - \left(^{206}pb/^{207}Pb\right)_{natural}} \times 100 \quad (2)$$

where $Pb_{anthropogenic}$ represents the contribution of a possible anthropogenic source in this mixing model, $(^{206}Pb/^{207}Pb)_{sample}$, $(^{206}Pb/^{207}Pb)_{natural}$, $(^{206}Pb/^{207}Pb)_{anthropogenic}$ are the isotopic signatures of PM_{10} samples, local natural background (in this case sediment, soil, sand and mine waste) and possible anthropogenic source (in this case exhausts from Pb-battery production industry), respectively. In the equation, only the $^{206}Pb/^{207}Pb$ ratio is written, however, similar binary mixing models can also be used for other Pb isotope ratios.

3. Results and discussion

3.1. Particle, Pb, and other potentially toxic elements concentrations

Concentrations of PM_{10} collected at five different locations in 2018 and 2021 are shown in Fig. 2. The highest particle concentration was determined in samples collected at Location #1 in June 2021. At that time, a high amount of desert dust was observed over the area, which most probably contributed to the increased PM_{10} concentration. The

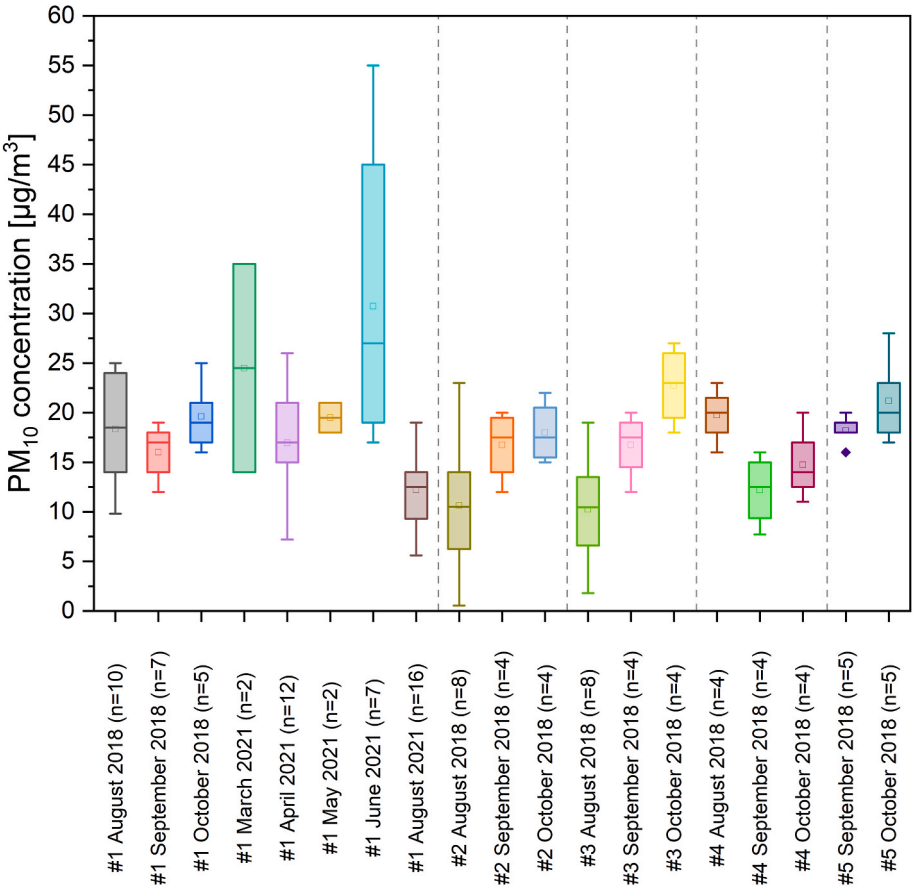

Fig. 2. Spatial and temporal distribution of PM_{10} concentration in the Upper Meža Valley.

limit concentration recommended by the World Health Organization for PM_{10} in the air is 45 µg/m^3 in 24 h and 15 µg/m^3 for the annual average (with only 3–4 exceedance days per year), while the annual limit value for Pb in airborne PM is 500 ng/m^3 (Directive, 2008, 2008; WHO global air quality guidelines, 2021). Of all the PM_{10} samples analysed, the daily limit value was exceeded only once at Location #1 in June 2021. Similarly, based on the daily measurements of PM_{10} at Location #1 by ARSO, the daily limit value was exceeded 6 times in the whole year, 2 times in June (Bec et al., 2022).

The average PTEs concentrations in PM_{10} at the majority of locations were in the following order Pb > Zn > Cd > As, except at Location #2, where Cd concentration was the lowest, and at Location #5, where Zn concentration was the highest (Fig. 3). The highest average Pb, and Cd concentrations were measured at Location #1 (ARSO monitoring station for PM_{10} particles in Žerjav), while the highest average Zn and As concentrations were measured at Location #2 and #5, respectively. The lowest average As and Cd concentrations were measured at Location #3. Žerjav is a settlement situated between steep hills, and the distances between the sampling locations are small, except for Location #5, which is in the neighbouring settlement. However, some differences in elemental compositions in the Žerjav measurement stations were detected. Location #4 is the closest to the mine waste deposit, while Locations #1 and #5 are closest to the secondary Pb production site in Žerjav and Črna na Koroškem, respectively. Based on their position, a greater influence from the production exhaust can be expected.

From Fig. 3, temporal differences may be observed for all four elements, however not significant. At Location #1, Pb and Zn concentrations were higher in 2021 compared to 2018, while this was not the case for As and Cd. The distribution of PM_{10} Pb concentrations was the largest among the analysed samples, showing large daily and spatial variability. The annual average Pb concentrations in PM_{10} at Location #1 increased from 300 ng/m^3 in 2009 to 694 ng/m^3 in 2021 (Ivartnik et al., 2022). In 2021 annual limit value was exceeded in 5 different months (Ivartnik et al., 2022). In June 2021, a high amount of desert dust was observed over the area, which caused increased concentrations of PM_{10} particles but did not influence the PTEs concentrations in the sampled particles. Similar trends can also be observed in graphs, where concentrations are calculated on the volume of sampled air (Fig. S2, Supplementary).

Total Pb, Zn, As, and Cd concentrations were also determined in soil, sand, sediments, ores, mine waste, and Pb-batteries. The elemental composition of Pb-batteries was used as a proxy for the exhaust from the battery production site. The results are presented in Table 1.

As expected, the highest Pb concentrations were found in Pb-battery components and Pb ores and minerals, followed by mine waste samples, sediments from the Meža River and its tributaries, and local sand and soil. The highest average Zn concentration was found in sphalerite, followed by galenite and mine waste. Since As and Cd are typically impurities in Pb and Zn ores, their concentrations were significantly lower than that of Pb. The highest average As concentration was detected in wulfenite, while the lowest was in Pb-grid from Pb-batteries. The highest average Cd concentration was found in sphalerite, with the lowest in Pb-paste samples 1, 2, and 3.

In soil Pb, Zn, As, and Cd concentrations were in the range of 32.6 mg/kg and 4153 mg/kg, 86.2 mg/kg and 6976 mg/kg, 6.13 mg/kg and 106 mg/kg, and 0.418 mg/kg and 46.1 mg/kg, respectively, and in sediments, between 114 mg/kg and 15609 mg/kg, 375 mg/kg and 15956 mg/kg, 10.3 mg/kg and 56.5 mg/kg, and 2.45 mg/kg and 88.0 mg/kg, respectively. The PTEs concentrations in the soil varied largely because some of the samples were taken at locations that underwent overlay with the uncontaminated soil. PTEs present in the soil are mostly a consequence of their release from mining and smelting activities that

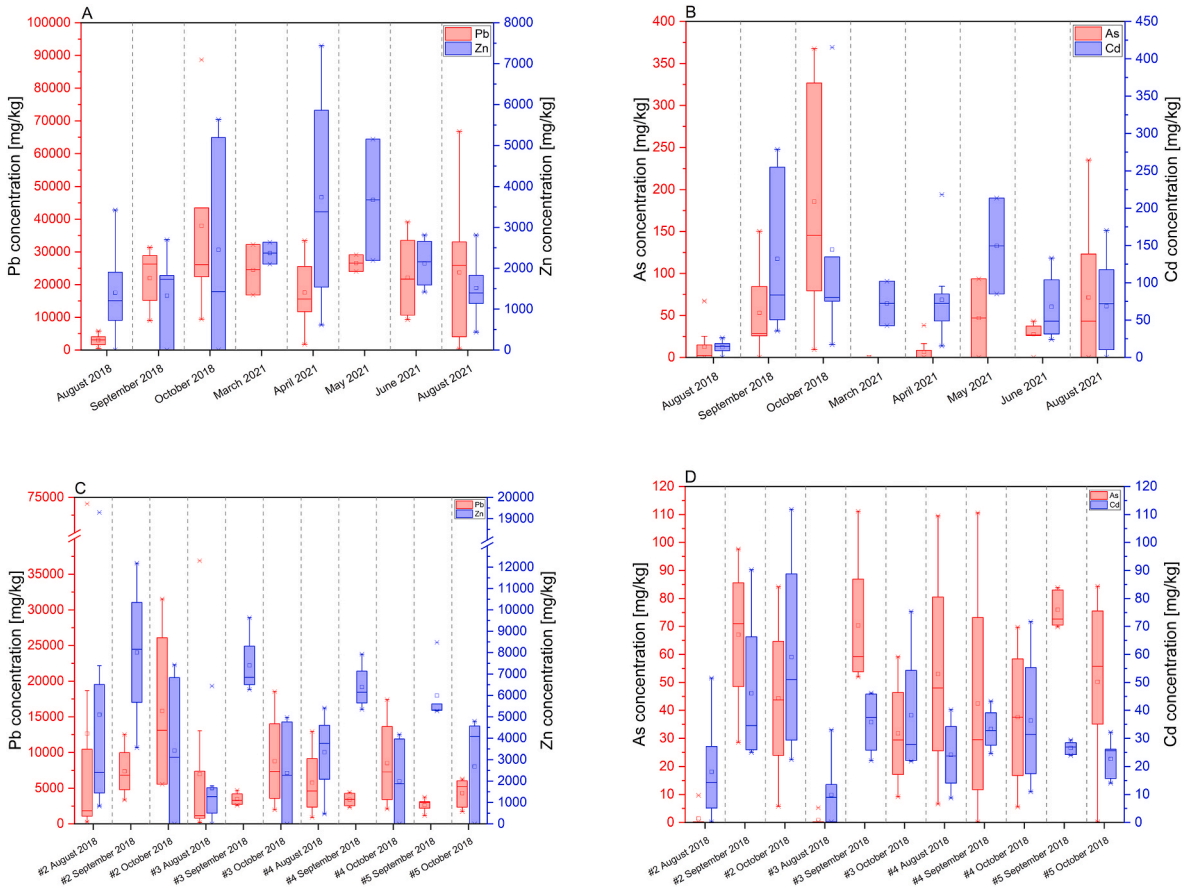

Fig. 3. Temporal and spatial variations of Pb, Zn, As, and Cd concentrations in PM_{10} samples. Figures A and B show Pb and Zn, and As and Cd concentrations at Location #1, respectively. Figures C and D show Pb and Zn, and As and Cd concentrations at Locations #2, #3, #4, and #5, respectively.

occurred for centuries, as well as a result of bedrock rich with Pb and Zn ore (Žibret et al., 2018), while in sediments of Meža River and its tributaries, mine waste deposits represent a significant source, as shown in the study of Miler and Gosar (2012) (Miler and Gosar, 2012). Compared to published data for PTEs in soil and sediment from the Upper Meža Valley, the concentrations did not change significantly through the years (Finzgar et al., 2014; Gosar and Miler, 2011). The comparison is reported in the Supplementary.

3.2. Enrichment factor (EF)

To estimate the potential anthropogenic input of Pb, Zn, Cd, and As in PM_{10} samples from the Upper Meža Valley, the enrichment factor (EF) was calculated (Table 2). Although the mean upper continental crust values provided by Wedepohl (1995) are typically used for calculating $(X/Fe)_{crust}$, this study adopted a different approach. Given the Upper Meža Valley's extensive history of Pb-ore mining and smelting, the local soil exhibits elevated concentrations of Pb, Zn, Cd, and As. Consequently, the average concentration values from all measured samples of the local soil were used to calculate the $(X/Fe)_{crust}$.

The lowest EF values were observed for Zn, followed by As. EF values below 10 suggested that the contribution to Zn and As was primarily from a crustal source, most likely from dust formed from the local soil. Higher EF values were observed for Cd and Pb, indicating a mixed source from both crustal and anthropogenic origins.

Examining the EFs for different months at Location #1, all four elements had EFs below 10 in August 2018. The EF for Zn remained below 10 in all other months, while As exhibited similar behaviour, except for October 2018 and August 2021, when the EF ranged between 10 and 100. The EF for Cd consistently ranged between 10 and 100 across all other months. The EF for Pb exceeded 100 in October 2018 and March 2021, but fluctuated between 10 and 100 in other months. The EF values, particularly for Pb, showed high variability within and between months. For instance, the EF for Pb at Location #1 was below 10 in August 2018, but in August 2021 it was above 60. In 2018, 9.09 % of all the PM_{10} samples from Location #1 had EFs for Pb exceeding 100, which increased to 20.5 % in 2021, indicating a rising anthropogenic input.

Numerous investigations of mining districts indicate that even when natural ore-related Pb concentrations are already elevated, historical mining and smelting activities further amplified the levels of PTEs, such as Pb, Zn, Cd, and As, in soils and airborne particulates (Mourinha et al., 2022; Svete et al., 2001). In the Upper Meža Valley specifically, earlier studies have demonstrated that the primary source of Pb, Zn, Cd, and As in soils is past mining and smelting operations, which redistributed ore and mine-waste material into the surface environment (Miler and Gosar, 2012; Žibret et al., 2018). The present results are consistent with these findings, confirming that natural ore mineralisation establishes a high geogenic baseline, while anthropogenic processing (secondary Pb production) has intensified the PTEs, especially Pb, burden in PM_{10}.

3.3. Lead isotope composition

Previous research in the Upper Meža Valley has predominantly concentrated on PTEs distribution and the environmental burden (Finzgar et al., 2014; Goltnik et al., 2022; Gosar and Miler, 2011; Miler and Gosar, 2019). Some data on Pb isotope ratios have been previously reported (Miler et al., 2022; Miler and Gosar, 2019; Wagner et al., 2022), however, a comprehensive source apportionment of Pb in PM_{10} with the use of Pb isotopes and evaluation of the contributions of individual sources has not yet been performed. Based on the previous discussion,

Table 1
Total PTEs concentrations determined in different types of samples collected in the Upper Meža Valley.

Sample Type	Number of samples	Conc. Pb [mg/kg]				Conc. Zn [mg/kg]				Conc. Cd [mg/kg]				Conc. As [mg/kg]			
		min	max	average	mean	min	max	average	mean	min	max	average	mean	min	max	average	mean
PM_{10}-Location #1*	61	350	88689	20025	18992	<1.48	7439	2159	1777	<0.239	415	77.5	67.3	<0.231	368	48.1	20.6
PM_{10}-Location #2*	16	256	74098	12124	5569	<1.48	19290	5409	4590	<0.239	112	35.3	25.9	<0.231	97.6	28.6	7.73
PM_{10}-Location #3*	16	184	36891	6552	2747	<1.48	9633	3281	1692	<0.239	75.3	23.4	22.0	<0.231	111	26.0	7.21
PM_{10}-Location #4*	12	900	17400	5899	4290	<1.48	7927	3906	3990	8.74	71.7	31.3	29.4	<0.231	111	44.4	40.1
$PM_{2.5}$-Location #4*	12	575	7262	3302	3205	5554	13716	9408	8694	<0.239	68.4	28.6	22.3	<0.231	195	64.6	75.2
PM_{10}-Location #5*	10	1165	6284	3482	3057	<1.48	8475	4340	5034	14.0	32.2	24.6	25.8	<0.231	84.4	63.1	71.6
Road dust*	3	208	260	229	217	908	1010	965	978	4.31	5.03	4.76	4.93	11.3	12.7	11.9	11.7
Sediment*	10	114	15609	4341	2405	375	15956	4616	3710	2.45	88.0	25.4	17.3	10.3	56.5	26.8	25.5
Soil*	26	32.6	4153	934	636	86.2	6976	1783	897	<0.239	46.1	10.9	4.78	6.13	106	23.0	20.1
Sand*	11	48.0	11179	2607	1515	554	30004	8125	6352	6.25	118	40.7	29.8	6.10	113	30.5	20.1
Mine waste*	4	578	28409	11994	9495	1281	88484	27711	10541	3.80	364	119	54.4	9.10	123	54.1	42.0
Wulfenite**	9	288006	621948	463745	563668	52.6	1232	375	218	1.91	15.3	8.56	7.98	733	1634	1169	1157
Galenite**	10	108187	916816	627484	585669	2401	114792	47196	41489	33.3	593	254	216	8.74	504	127	52.1
Sphalerite**	1			3703				691608				3408				148	
Slate**	2	90.2	95.5	92.9	92.9	2182	2213	2197	2197	4.37	4.49	4.43	4.43	16.7	17.0	16.8	16.8
Andesite**	2	115	581	348	348	91.3	149	120	120	<0.239	<0.239	<0.239	<0.239	1.51	2.14	1.83	1.83
Basalt**	2	44.2	66.9	55.6	55.6	169	175	172	172	<0.239	<0.239	<0.239	<0.239	3.15	3.17	3.16	3.16
Pb-grid*	5	561234	726716	632046	605751	<1.48	<1.48	<1.48	<1.48	19.6	52.3	34.4	29.6	<0.231	0.551	0.295	0.231
Pb-paste 1*	6	342742	693744	528714	552949	<1.48	<1.48	<1.48	<1.48	<0.239	0.532	0.358	0.341	<0.231	5.70	1.26	0.231
Pb-paste 2*	6	326514	645829	469625	479761	<1.48	<1.48	<1.48	<1.48	<0.239	0.287	0.260	0.255	<0.231	4.59	1.33	0.563
Pb-paste 3*	6	229887	805259	514034	495270	<1.48	<1.48	<1.48	<1.48	<0.239	0.414	0.341	0.355	<0.231	6.22	1.47	0.521

* Present study

** Personal communication [45]

Table 2
Enrichment factors (EF) for Pb, Zn, As, and Cd in PM_{10} and $PM_{2.5}$ samples collected in the Upper Meža Valley at 5 locations in 2018 and 2021. EF values below 10 are marked with green colour, EF values between 10 and 100 are marked with orange colour, and EF values above 100 are marked with red colour.

Location	Month	EF			
		Pb	Zn	As	Cd
#1 PM_{10}	August 2018	8.56 ± 4.84	1.91 ± 1.32	2.03 ± 3.52	3.27 ± 1.64
	September 2018	69.1 ± 18.3	2.16 ± 1.89	8.03 ± 7.37	33.6 ± 21.1
	October 2018	151 ± 129	5.42 ± 6.32	38.2 ± 33.8	49.0 ± 52.5
	March 2021	105 ± 78	4.63 ± 0.97	0.045 ± 0.016	26.8 ± 23.0
	April 2021	62.5 ± 28.2	7.56 ± 6.44	0.702 ± 1.255	23.0 ± 10.1
	May 2021	75.8 ± 36.8	5.74 ± 4.85	4.84 ± 6.78	31.4 ± 8.7
	June 2021	54.4 ± 42.7	2.47 ± 1.38	2.96 ± 2.31	15.2 ± 13.6
	August 2021	66.1 ± 44.8	2.50 ± 1.15	10.6 ± 11.7	16.9 ± 13.8
#2 PM_{10}	August 2018	5.69 ± 6.72	2.31 ± 0.91	0.159 ± 0.394	2.31 ± 2.54
	September 2018	13.4 ± 6.3	8.05 ± 4.69	6.66 ± 4.10	6.85 ± 2.94
	October 2018	64.5 ± 76.8	5.38 ± 6.22	7.95 ± 5.73	20.2 ± 22.3
#3 PM_{10}	August 2018	10.9 ± 15.1	1.67 ± 1.16	0.115 ± 0.241	2.35 ± 2.52
	September 2018	9.90 ± 4.31	11.0 ± 5.0	10.1 ± 5.2	8.58 ± 4.00
	October 2018	58.9 ± 56.1	10.1 ± 11.9	12.1 ± 10.9	21.6 ± 16.9
#4 PM_{10}	August 2018	13.8 ± 8.4	4.58 ± 3.02	6.50 ± 4.01	5.68 ± 3.22
	September 2018	16.2 ± 5.8	15.5 ± 4.7	9.51 ± 10.98	13.4 ± 3.9
	October 2018	63.5 ± 67.4	7.73 ± 9.06	14.4 ± 11.6	23.9 ± 22.0
#4 $PM_{2.5}$	August 2018	16.1 ± 9.7	22.5 ± 6.2	18.5 ± 3.1	9.65 ± 8.14
	September 2018	13.5 ± 2.9	28.1 ± 4.3	0.074 ± 0.015	11.0 ± 2.0
	October 2018	25.8 ± 22.3	25.1 ± 8.2	29.8 ± 15.0	21.7 ± 12.7
#5 PM_{10}	September 2018	12.2 ± 4.2	14.3 ± 3.6	17.6 ± 1.8	10.6 ± 1.5
	October 2018	23.3 ± 15.3	9.50 ± 9.83	16.8 ± 10.5	11.7 ± 6.2

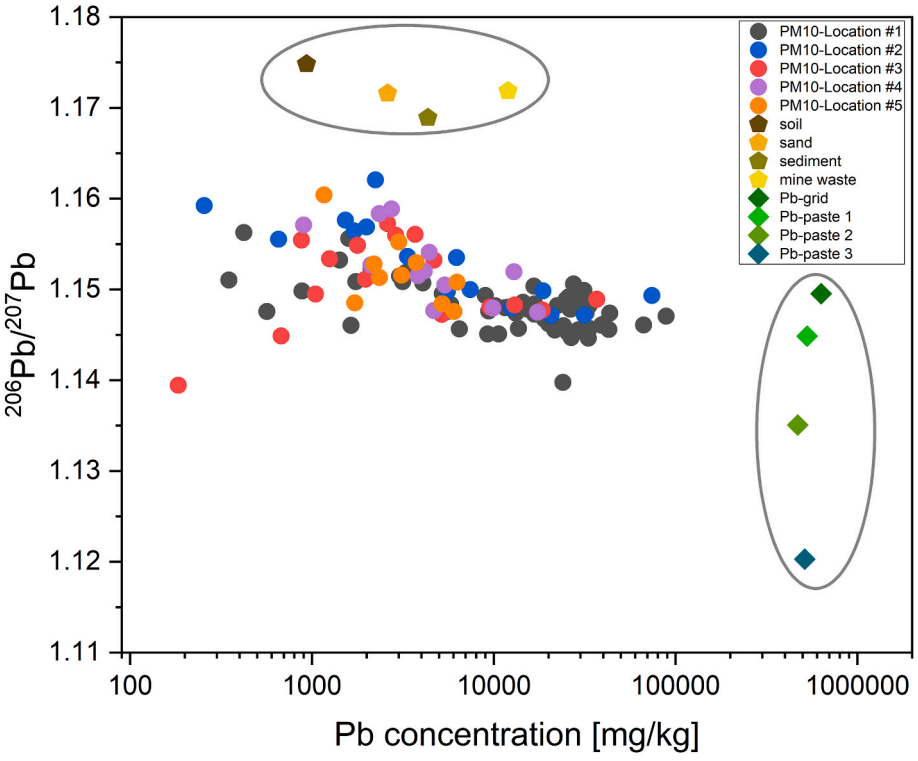

Fig. 4. $^{206}Pb/^{207}Pb$ isotope ratios and Pb concentrations (log scale) of PM_{10} samples and potential Pb emission sources.

the Pb sources in PM_{10} samples couldn't be determined based on total PTEs concentrations. Therefore, Pb isotope composition was determined in PM_{10}, and different samples from the Upper Meža Valley were identified as potential Pb sources. The Pb isotope ratios and concentrations in PM_{10}, soil, sand, sediments, mine waste and Pb-battery components are shown in Fig. 4. The $^{206}Pb/^{207}Pb$ *vs.* [Pb] displays the separation of two different sources of Pb. One comes from the background environment ($^{206}Pb/^{207}Pb$ between 1.162 and 1.183) and the other from the secondary Pb production industry ($^{206}Pb/^{207}Pb$ between 1.120 and 1.153).

The distribution of Pb isotope ratio values in the PM_{10} particles between the geogenic and anthropogenic sources is even more pronounced in the biplots of $^{208}Pb/^{206}Pb$ *vs.* $^{206}Pb/^{207}Pb$, $^{208}Pb/^{204}Pb$ *vs.* $^{207}Pb/^{204}Pb$, and $^{208}Pb/^{204}Pb$ *vs.* $^{206}Pb/^{204}Pb$, presented in Fig. 5, and Fig. S3 A, B (Supplementary), respectively. Pb isotope ratios for each sample of sediment, soil, sand, mine waste, ores, Pb-battery

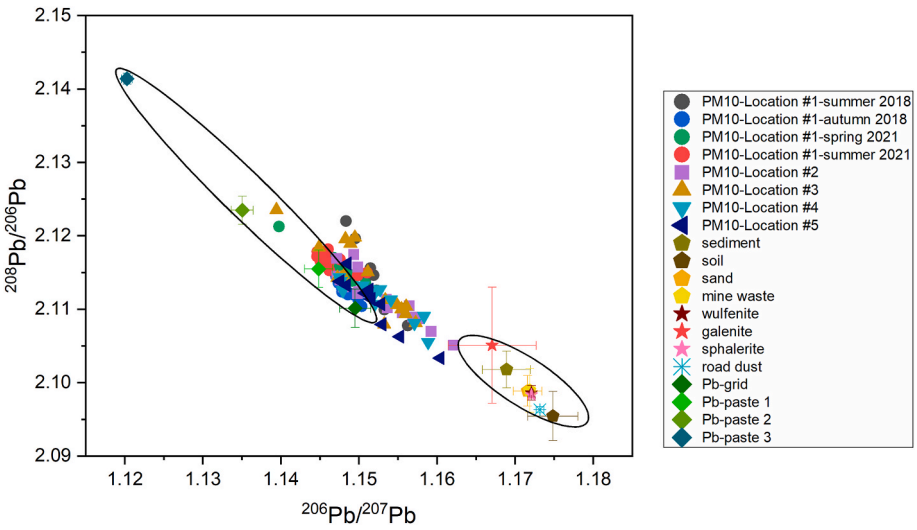

Fig. 5. Biplot of $^{208}Pb/^{206}Pb$ *vs.* $^{206}Pb/^{207}Pb$ for PM_{10} and possible emission source samples from the Upper Meža Valley.

components, PM_{10}, and $PM_{2.5}$ are shown in Table S5 (Supplementary).

On the bottom right side of the plot in Fig. 5 are local environmental/background samples, such as sediment, soil, sand, mine waste, and ores. The Meža Valley is known for its Pb-Zn ore deposits. The Mežica ore deposit is predominantly composed of primary sulphide minerals, secondary oxide, and sulphide minerals. The deposit is a "Mississippi Valley" type (MVT) Pb-Zn ore deposit that is hosted in the Middle/Upper-Triassic Wetterstein platform carbonates (Gosar and Miler, 2011). Pb isotope ratios in galenite ores were 1.162–1.173, 38.360–38.564, 15.614–15.683, 18.205–18.377, 2.094–2.113, and for wulfenite 1.172–1.173, 38.456–38.574, 15.644–15.679, 18.344–18.374, 2.096–2.099 for $^{206}Pb/^{207}Pb$, $^{208}Pb/^{204}Pb$, $^{207}Pb/^{204}Pb$, $^{206}Pb/^{204}Pb$, $^{208}Pb/^{206}Pb$, respectively (Fig. 5) (Rogan Šmuc et al., 2025). Pb isotope ratios of galenite ores were in good agreement with the values reported by Miler and Gosar (2019) (Miler and Gosar, 2019), which were 38.5, 15.7, and 18.4 for $^{208}Pb/^{204}Pb$, $^{207}Pb/^{204}Pb$, and $^{206}Pb/^{204}Pb$, respectively (Miler and Gosar, 2019). Mine waste is a mixture of Pb from different ores, and its isotope ratios are similar to those of galenite and wulfenite ores. Pb isotope ratios of mine waste determined in this study were in good agreement with the values reported by Miler et al. (2022) (Miler et al., 2022), who investigated the environmental impact of mine waste deposits in Slovenia. They analysed mine waste samples from the Upper Meža Valley, Litija, and Pleše. The reported $^{208}Pb/^{204}Pb$, $^{207}Pb/^{204}Pb$, and $^{206}Pb/^{204}Pb$ ratios in three mine waste samples from the Upper Meža Valley were 38.7, 15.8, and 18.5–18.8, respectively (Miler et al., 2022).

Since most of the analysed soils were of local origin, their Pb isotope ratios were similar to those of ores and mine waste, indicating that Pb smelting was an important source of Pb in soil. Pb isotope ratios of soils were in good agreement with the values reported by Wagner et al. (2022) (Wagner et al., 2022), who investigated the use of selective diffusive gradients in thin films for the simultaneous determination of Sr and Pb concentrations and isotope ratios in soils. The reported $^{206}Pb/^{207}Pb$, $^{208}Pb/^{204}Pb$, $^{207}Pb/^{204}Pb$, $^{206}Pb/^{204}Pb$, and $^{208}Pb/^{206}Pb$ ratios were 1.172, 38.517, 15.663, 18.360, and 2.098, respectively (Wagner et al., 2022). However, in this study, some samples were collected from sites where the soil was exchanged (playgrounds, surroundings of kindergartens and schools). Their non-local origin was evident mostly from their lower Pb concentrations (30–70 mg/kg) as well as from their slightly different values of Pb isotope ratios, which were 1.182, 38.792, 15.708, 18.568, 2.089 for $^{206}Pb/^{207}Pb$, $^{208}Pb/^{204}Pb$, $^{207}Pb/^{204}Pb$, $^{206}Pb/^{204}Pb$, $^{208}Pb/^{206}Pb$, respectively. These results are in agreement with findings by Ettler et al. (2004) (Ettler et al., 2004), who investigated soils that were heavily contaminated by Pb smelting. Samples were collected near a Pb smelter in Příbram (Czech Republic), where smelting of local ores was replaced by smelting of old Pb-batteries. Based on the Pb isotope composition and endmember mixing model, all of the Pb in topsoil was attributed to Pb from battery processing, and Pb from ore processing prevailed at a depth of 10 cm. The authors concluded that Pb smelting had the biggest impact on the contamination of soils in the area (Ettler et al., 2004). Similarly, Mackay et al. (2013) (Mackay et al., 2013) used Pb isotopes to determine the source and pathway of Pb in soil, household dust, and aerosols from a Cu and Pb mining and smelting city in Australia, Mount Isa. The Pb isotope ratios confirmed that the dominant source of Pb contamination was from mining and smelting emissions (Mackay et al., 2013).

On the upper left side of the plot in Fig. 5, the Pb isotope compositions of Pb-battery components are plotted, with $^{208}Pb/^{206}Pb$ and $^{206}Pb/^{207}Pb$ ratios ranging from 2.107 to 2.142, and from 1.120 to 1.153, respectively. Their Pb isotope ratio variability was higher than that of local environmental samples, as recycled Pb can come from different locations/parts of the world, which can have different Pb isotope compositions (Wang et al., 2021).

The road dust had a Pb isotope composition similar to that of soil and mine waste, while the PM_{10} samples slightly differed from the local (background) samples and had the $^{208}Pb/^{206}Pb$ and $^{206}Pb/^{207}Pb$ isotope ratios ranging between 2.103 and 2.124, and from 1.139 to 1.162, respectively. They were situated between the two end members. A similar grouping was also observed in biplots of $^{208}Pb/^{204}Pb$ *vs.* $^{207}Pb/^{204}Pb$ and $^{208}Pb/^{204}Pb$ *vs.* $^{206}Pb/^{204}Pb$.

3.3.1. *Spatial and temporal variability*

The PM_{10} particles were sampled at 5 locations, of which 4 were in the same settlement (Žerjav) and one was from Črna na Koroškem. Both settlements were affected by mining activities in the valley as well as by the exhausts from industry related to the secondary Pb production. Therefore, the concentration levels of PTEs and the Pb isotope composition in PM_{10} were similar between them. Also, between samples from Žerjav (Location #1, #2, #3, and #4), no difference was observed between those closer to the mine waste deposit and those near the secondary Pb production factory. Present observations do not agree with the findings from the study about particles in snow from the same region, where the authors found that the influence of the source decreases with distance (Miler and Gosar, 2013). The discrepancy between the findings may be attributed first to the size of the studied particles, as smaller particles may travel longer distances than the bigger ones, and secondly to the season of sampling, as precipitation can wash the atmosphere and contribute to quicker settlement of the particles.

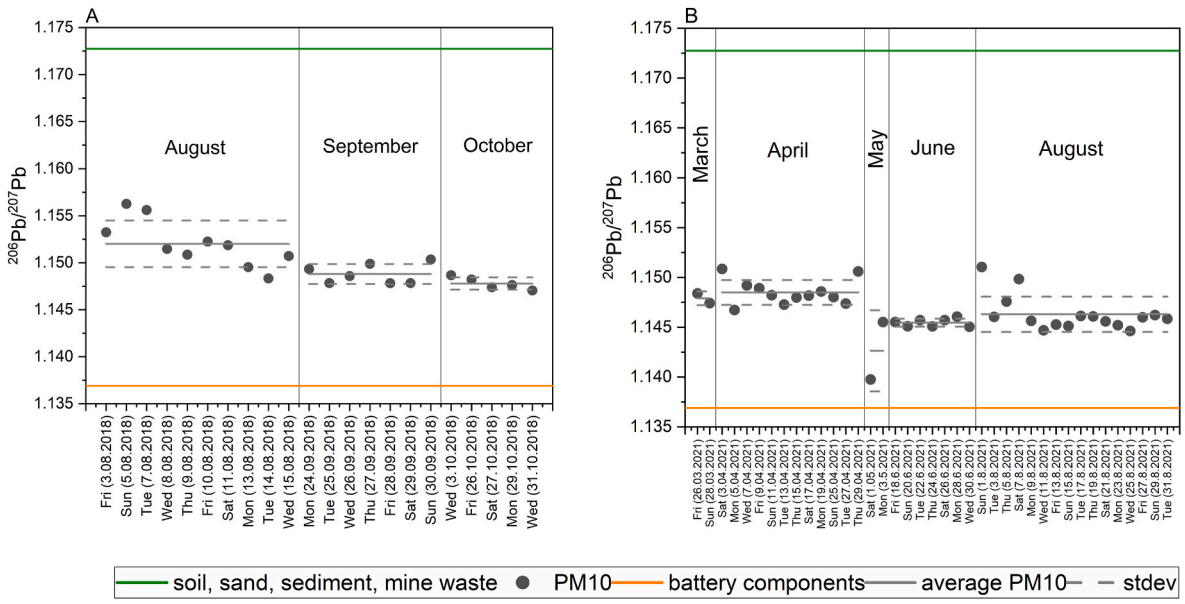

Fig. 6. Temporal variability of $^{206}Pb/^{207}Pb$ isotope ratio in PM_{10} samples at Location #1 in A) 2018 and B) 2021.

Contrary to spatial variability, some temporal differences were observed at Location #1 (PM_{10} monitoring station), although small, they were significant ($p < 0.05$) (Fig. 6).

Fig. 6 shows slight monthly variability in both years. In 2018, the Pb isotope ratio values were closer to the background values compared to 2021. In September and October 2018, Pb isotope ratio values were closer to anthropogenic values compared to August, likely due to the summer holidays in August and the resulting decrease in secondary Pb production. At the beginning of 2021 (March and April), the COVID-19 restrictions may have caused the PM_{10} Pb isotope composition to lean towards background values compared to June and the second half of August, when the Pb isotope ratio values were lower and closer to anthropogenic values. Notably, in June, despite a significant influx of desert dust increasing particle concentration, the isotope composition of PM_{10} samples remained unchanged.

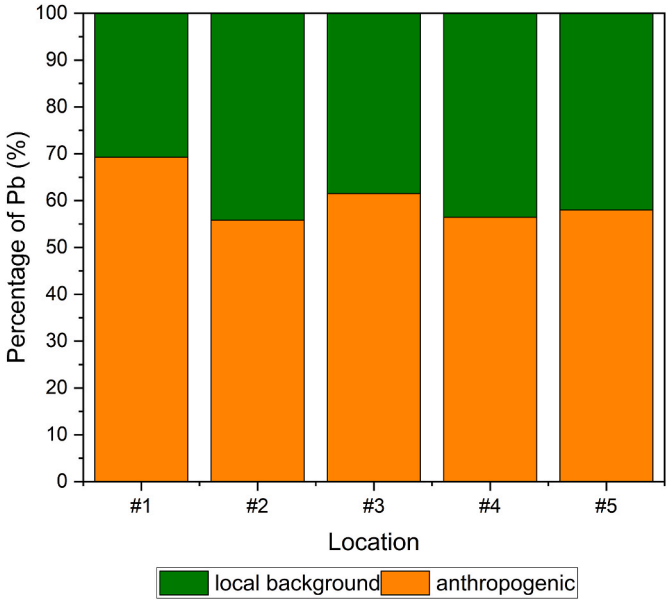

Fig. 7. The percent contribution to Pb in PM_{10} from two sources, the anthropogenic source and local background.

3.3.2. *Comparison of PM_{10} and $PM_{2.5}$*

At Location #4, both PM_{10} and $PM_{2.5}$ particulate matter samples were collected independently to assess differences in total elemental concentrations (Fig. S4 (Supplementary)) and Pb isotope composition (Fig. S5 (Supplementary)). While daily fluctuations were observed in the concentrations of Pb, As, and Cd, statistical analysis revealed no significant differences ($p > 0.05$) in the average concentrations of these elements between the two particulate size fractions. This suggests that the sources and atmospheric behaviour of these elements may be similar across coarse and fine particulate matter, which is similar to findings in smaller urban environments (Chatoutsidou and Lazaridis, 2022) and contrary to findings in megacities, where more of the different industries can be present (Hao et al., 2018; Zhang et al., 2018). In contrast, Zn exhibited a significantly higher average concentration in $PM_{2.5}$ than in PM_{10} ($p < 0.05$), indicating a possible enrichment in finer particles. This is likely due to Zn's strong association with combustion-related processes, particularly from vehicular emissions, which predominantly contribute to the fine particle fraction (Pant et al., 2017; Pant and Harrison, 2012). When comparing average enrichment factors for Pb, Zn, As, and Cd in two particulate fractions, only the average EF for Zn showed significantly higher enrichment in the $PM_{2.5}$ fraction ($p < 0.05$).

When comparing Pb isotope ratios between PM_{10} and $PM_{2.5}$, no significant differences were observed ($p > 0.05$), suggesting a common source, a well-mixed origin of Pb in both fractions, or that Pb could be primarily found within the finer particle range. This aligns with studies that have shown isotopic homogeneity in Pb across different particle sizes in urban atmospheres, particularly where industrial or legacy sources dominate (Hu et al., 2014; Souto-Oliveira et al., 2018).

3.3.3. *Estimation of Pb source's contribution by the mixing model*

From the data presented so far, an exclusive origin of Pb only from the local background can be ruled out. To estimate the contributions of different sources of Pb in the PM_{10} samples, an endmember mixing model was adopted (Monna et al., 1997). In this study, two possible sources were identified, local background samples (sediment, soil, sand, mine waste) and an additional anthropogenic source (secondary Pb production industry). As it was not possible to determine individual Pb contributions to PM_{10} based on Pb isotope composition from sediment, soil, sand, and mine waste, as they have very similar isotope composition, these samples were grouped as local background samples. On the other hand, the anthropogenic source had a different Pb isotope

composition. With the use of the $^{206}Pb/^{207}Pb$ ratio, the percent contribution to Pb in PM_{10} from anthropogenic source was calculated (Fig. 7) and was around (69.3 ± 7.8) % at Location #1, (55.8 ± 13.3) % at Location #2, (61.5 ± 13.5) % at Location #3, (56.4 ± 11.1) % at Location #4, and (58.0 ± 10.6) % at Location #5. The results showed that both background and anthropogenic sources contribute to Pb in PM_{10}, however, the anthropogenic one prevailed. Similar results were obtained for other Pb isotope ratios. These results confirmed the assumption from the elemental composition of the PM_{10} at Location #1 to have a greater influence from the Pb-battery production exhaust, as it is situated nearby.

The anthropogenic contribution of Pb to PM at Location #4 was similar between PM_{10} and $PM_{2.5}$, the second being slightly but not significantly higher ($p > 0.05$), at (57.0 ± 11.2) %.

The data presented in this study indicated a substantial contribution of anthropogenic sources to Pb in PM_{10} particles, with anthropogenic Pb accounting for between 55.8 % and 69.3 % across various locations. This highlights secondary Pb production, particularly from current activities such as Pb recycling and battery production, as a major source of atmospheric Pb today. A study on mineralogical and elemental composition of snow deposits from the same region found that although approximately 85 % of PTE-bearing particles originated from present-day Pb recycling, these particles represented only about 8.5 % of all deposited particles (Miler and Gosar, 2013; Žibret et al., 2018). This suggests that, nearly two decades ago, secondary Pb production had a relatively minor influence on overall environmental contamination, with legacy sources, such as historically deposited mine waste, still playing a significant role in contributing Pb-enriched particles to the atmosphere. The differences observed between the two studies can be attributed to several interrelated factors. First, the sampling periods differed significantly: Miler and Gosar (2013) (Miler and Gosar, 2013) collected samples in February 2009, while the present study gathered samples in August, September, and October of 2018 and March, April, May, June, and August of 2021. Over the intervening decade, activities related to battery recycling and production, and the availability of recycled materials, are likely to have increased. Methodological differences also play a role; Miler and Gosar (2013) (Miler and Gosar, 2013) employed SEM-EDS, whereas the present study used Pb isotope composition and an end-member mixing model, which may capture different aspects of Pb pollution. Furthermore, the two studies defined and categorised Pb sources differently. Miler and Gosar (2013) (Miler and Gosar, 2013) distinguished between present-day Pb recycling and historical sources, while the current study grouped soil, sand, and mine waste into a broader local environmental or background category. These differences in analytical approach, time of sampling, and source classification highlight the complexity of tracing Pb pollution and underscore the need to address both historical and contemporary sources of environmental Pb contamination. However, Pb isotopes were proven as a reliable tool for source apportionment of PM_{10}, especially in areas with mining and smelting industries. For example, they were used by Félix et al. (2015) (Félix et al., 2015), who investigated sources of atmospheric aerosol in the mining site in Hayden (Arizona, USA), which has a concentrator, smelter, and tailing facilities, and there are also various mines in the vicinity. The study was performed in two towns with a small population that are located in this area. The Pb isotope ratios revealed two different sources, the first originating from condensation of high-temperature vapours emitted from the smelter, and the second related to the background Pb present in the area (Félix et al., 2015).

4. Conclusions

This study applied multielemental and Pb isotope analysis to investigate the sources of PM_{10} in the Upper Meža Valley, a historically contaminated region in northeastern Slovenia. Concentrations of PTEs were the highest for Pb, followed by Zn, Cd, and As, with only minor temporal variability observed. An increase in Pb and Zn levels was detected at one site in 2021 relative to 2018, while As and Cd remained relatively stable over time.

For the first time in this region, Pb isotope ratios were utilized for detailed source apportionment of PM_{10}. Local environmental materials, including sediment, soil, sand, mine waste, and ores, displayed similar isotopic signatures, consistent with their shared origin from the Mississippi Valley-type (MVT) Pb-Zn ore deposit. In contrast, Pb-battery components exhibited a broader range of isotope ratios, reflecting their more heterogeneous and global sources. PM_{10} samples collected from Žerjav and Črna na Koroškem showed similar Pb isotope compositions intermediate between environmental and anthropogenic end-members. The results demonstrated that Pb in PM_{10} originated from both geogenic and anthropogenic sources, with a substantial portion attributed to contemporary human activities, particularly in the vicinity of battery production sites. These findings emphasize the importance of combining elemental and isotopic techniques for accurate source apportionment, especially in regions with a legacy of industrial pollution. While this study focused on the Upper Meža Valley, its methodological approach and implications are broadly relevant for other regions worldwide facing similar environmental and health challenges.

CRediT authorship contribution statement

Tjaša Žerdoner: Writing – original draft, Visualization, Methodology, Investigation, Formal analysis, Data curation, Conceptualization. **Judita Burger:** Writing – review & editing, Conceptualization. **Irena Kranjc:** Writing – review & editing, Conceptualization. **Janja Turšič:** Writing – review & editing, Conceptualization. **Tea Zuliani:** Writing – review & editing, Visualization, Validation, Supervision, Resources, Project administration, Methodology, Investigation, Funding acquisition, Data curation, Conceptualization.

Declaration of competing interest

The authors declare that they have no known competing financial interests or personal relationships that could have appeared to influence the work reported in this paper.

Acknowledgements

This research was funded by the Slovenian Research and Innovation Agency – ARIS: Program (P1-0143), Young researcher program (PR-10487), CRP Project – Identification of Pb sources in the Upper Meža Valley based on Pb isotope composition (V1-1939), and research project DISCOVER (J1-60008, PIN8195924), together with Austrian Science Fund – FWF.

Appendix A. Supplementary data

Supplementary data to this article can be found online at https://doi.org/10.1016/j.atmosenv.2025.121666.

Data availability

Data will be made available on request.

References

Beane, S.J., Comber, S.D.W., Rieuwerts, J., Long, P., 2016. Abandoned metal mines and their impact on receiving waters: a case study from Southwest England. Chemosphere 153, 294–306.

Bec, D., Ciglenečki, D., Dolšak Lavrič, P., Gjerek, M., Koleša, T., Logar, M., et al., 2022. Kakovost Zraka V Sloveniji V Letu 2021. ARSO, Ljubljana.

Bodor, K., Micheu, M.M., Keresztesi, Á., Birsan, M.V., Nita, I.A., Bodor, Z., et al., 2021. Effects of PM10 and weather on respiratory and cardiovascular diseases in the ciuc Basin (Romanian carpathians). Atmosphere 12 (2), 289.

Bollhöfer, A., Rosman, K.J.R., 2001. Isotopic source signatures for atmospheric lead: the Northern Hemisphere. Geochem. Cosmochim. Acta 65 (11), 1727–1740.

Cesari, D., Contini, D., Genga, A., Siciliano, M., Elefante, C., Baglivi, F., et al., 2012. Analysis of raw soils and their re-suspended PM10 fractions: characterisation of source profiles and enrichment factors. Appl. Geochem. 27 (6), 1238–1246.
Chatoutsidou, S.E., Lazaridis, M., 2022. Mass concentrations and elemental analysis of PM2.5 and PM10 in a coastal Mediterranean site: a holistic approach to identify contributing sources and varying factors. Sci. Total Environ. 838, 155980.
Csavina, J., Field, J., Taylor, M.P., Gao, S., Landázuri, A., Betterton, E.A., et al., 2012. A review on the importance of metals and metalloids in atmospheric dust and aerosol from mining operations. Sci. Total Environ. 433, 58–73.
Dewan, N., Majestic, B.J., Ketterer, M.E., Miller-Schulze, J.P., Shafer, M.M., Schauer, J.J., et al., 2015. Stable isotopes of lead and strontium as tracers of sources of airborne particulate matter in Kyrgyzstan. Atmos. Environ. 120, 438–446.
Di Girolamo, P., 2020. Assessment of the potential role of atmospheric particulate pollution and airborne transmission in intensifying the first wave pandemic impact of SARS-CoV-2/COVID-19 in Northern Italy. Bull. Atmos Sci. Technol. 1 (3–4), 515–550.
Directive 2008/50/EC of the European Parliament and of the Council of 21 May 2008 on Ambient Air Quality and Cleaner Air for Europe, 2008. European Union.
Dong, S., Ochoa Gonzalez, R., Harrison, R.M., Green, D., North, R., Fowler, G., et al., 2017. Isotopic signatures suggest important contributions from recycled gasoline, road dust and non-exhaust traffic sources for copper, zinc and lead in PM10 in London, United Kingdom. Atmos. Environ. 165, 88–98.
Doufexi, M., Gamvroula, D.E., Alexakis, D.E., 2022. Elements' content in stream sediment and wildfire ash of suburban areas in West Attica (Greece). Water 14 (3), 310.
EN 14902 Ambient air quality, 2005. Standard Method for the Measurement of Pb, Cd, As, and Ni in the PM10 Fraction of Suspended Particulate Matter.
Enamorado-Báez, S.M., Gómez-Guzmán, J.M., Chamizo, E., Abril, J.M., 2015. Levels of 25 trace elements in high-volume air filter samples from Seville (2001–2002): sources, enrichment factors and temporal variations. Atmos. Res. 155, 118–129.
Entwistle, J.A., Hursthouse, A.S., Marinho Reis, P.A., Stewart, A.G., 2019. Metalliferous mine dust: human health impacts and the potential determinants of disease in mining communities. Curr. Pollut. Rep. 5 (3), 67–83.
Ettler, V., 2016. Soil contamination near non-ferrous metal smelters: a review. Appl. Geochem. 64, 56–74.
Ettler, V., Mihaljevic, M., Komárek, M., 2004. ICP-MS measurements of lead isotopic ratios in soils heavily contaminated by lead smelting: tracing the sources of pollution. Anal. Bioanal. Chem. 378 (2), 311–317.
European environment agency glossary [Internet] [cited 2025 Oct 10]. Available from: https://www.eea.europa.eu/help/glossary/eea-glossary.
Faraji, M., Pourpak, Z., Naddafi, K., Nodehi, R.N., Nicknam, M.H., Shamsipour, M., et al., 2019. Chemical composition of PM10 and its effect on in vitro hemolysis of human red blood cells (RBCs): a comparison study during dust storm and inversion. J. Environ. Health Sci. Eng. 17 (1), 493–502.
Félix, O.I., Csavina, J., Field, J., Rine, K.P., Sáez, A.E., Betterton, E.A., 2015. Use of lead isotopes to identify sources of metal and metalloid contaminants in atmospheric aerosol from mining operations. Chemosphere 122, 219–226.
Finzgar, N., Jez, E., Voglar, D., Lestan, D., 2014. Spatial distribution of metal contamination before and after remediation in the Meza Valley, Slovenia. Geoderma 217–218, 135–143.
Goltnik, T., Burger, J., Kranjc, I., Turšič, J., Zuliani, T., 2022. Potentially toxic elements and Pb isotopes in mine-draining meža River catchment (NE Slovenia). Water 14 (7), 998.
Gosar, M., Miler, M., 2011. Anthropogenic metal loads and their sources in stream sediments of the Meža River catchment area (NE Slovenia). Appl. Geochem. 26 (11), 1855–1866.
Gošar, D., Costa, M.R., Ferreira, A., Štrucl, S.F., 2015. Assessment of past and present water quality in closed Mežica Pb-Zn Mine (Slovenia). Comunicações. Geológicas. 102 (1), 65–69.
Hao, Y., Meng, X., Yu, X., Lei, M., Li, W., Shi, F., et al., 2018. Characteristics of trace elements in PM2.5 and PM10 of Chifeng, northeast China: insights into spatiotemporal variations and sources. Atmos. Res. 213, 550–561.
Hu, X., Sun, Y., Ding, Z., Zhang, Y., Wu, J., Lian, H., et al., 2014. Lead contamination and transfer in urban environmental compartments analyzed by lead levels and isotopic compositions. Environ. Pollut. 187, 42–48.
Ivartnik, M., Pavlič, H., Hudopisk, N., Simetinger, M., Ploder, J., Kajnih, N., 2019. Poročilo o izvajanju programa ukrepov za izboljšanje kakovosti okolja v Zgornji Mežiški dolini za leto. Ravne, Koroškem, pp. 1–74.
Ivartnik, M., Pavlič, H., Hudopisk, N., Simetinger, M., Ploder, J., Hočevar, B., et al., 2022. Poročilo o izvajanju programa ukrepov za izboljšanje kakovosti okolja v Zgornji Mežiški dolini za leto. Ravne. Koroškem: NIJZ. Ravne. 2022.
Jez, E., Lestan, D., 2015. Prediction of blood lead levels in children before and after remediation of soil samples in the upper Meza Valley, Slovenia. J. Hazard Mater. 296, 138–146.
Kong, H., Teng, Y., Song, L., Wang, J., Zhang, L., 2018. Lead and strontium isotopes as tracers to investigate the potential sources of lead in soil and groundwater: a case study of the Hun River alluvial fan. Appl. Geochem. 97, 291–300.
Lee, S., Han, C., Shin, D., Hur, S.D., Jun, S.J., Kim, Y.T., et al., 2017. Characteristics of elemental and Pb isotopic compositions in aerosols (PM10-2.5) at the Ieodo Ocean Research Station in the East China Sea. Environ. Pollut. 231, 154–164.
Li, F.L., Liu, C.Q., Yang, Y.G., Bi, X.Y., Liu, T.Z., Zhao, Z.Q., 2012. Natural and anthropogenic lead in soils and vegetables around Guiyang city, southwest China: a Pb isotopic approach. Sci. Total Environ. 431, 339–347.
Li, F., Jinxu, Y., Shao, L., Zhang, G., Wang, J., Jin, Z., 2018. Delineating the origin of Pb and Cd in the urban dust through elemental and stable isotopic ratio: a study from Hangzhou City, China. Chemosphere 211, 674–683.
Mackay, A.K., Taylor, M.P., Munksgaard, N.C., Hudson-Edwards, K.A., Burn-Nunes, L., 2013. Identification of environmental lead sources and pathways in a mining and smelting town: mount Isa, Australia. Environ. Pollut. 180, 304–311.
Manalis, N., Grivas, G., Protonotarios, V., Moutsatsou, A., Samara, C., Chaloulakou, A., 2005. Toxic metal content of particulate matter (PM10), within the Greater Area of Athens. Chemosphere 60 (4), 557–566.
Miler, M., Gosar, M., 2012. Characteristics and potential environmental influences of mine waste in the area of the closed Mežica Pb–Zn mine (Slovenia). J. Geochem. Explor. 112, 152–160.
Miler, M., Gosar, M., 2013. Assessment of metal pollution sources by SEM/EDS analysis of solid particles in snow: a case Study of Žerjav, Slovenia. Microsc. Microanal. 19 (6), 1606–1619.
Miler, M., Gosar, M., 2019. Assessment of contribution of metal pollution sources to attic and household dust in pb-polluted area. Indoor Air 29 (3), 487–498.
Miler, M., Bavec, Š., Gosar, M., 2022. The environmental impact of historical Pb-Zn mining waste deposits in Slovenia. J. Environ. Manag. 308, 114580.
Monna, F., Lancelot, J., Croudace, I.W., Cundy, A.B., Lewis, J.T., 1997. Pb isotopic composition of airborne particulate material from France and the Southern United Kingdom: implications for Pb pollution sources in urban areas. Environ. Sci. Technol. 31 (8), 2277–2286.
Mourinha, C., Palma, P., Alexandre, C., Cruz, N., Rodrigues, S.M., Alvarenga, P., 2022. Potentially toxic elements' contamination of soils affected by mining activities in the Portuguese sector of the Iberian pyrite Belt and optional remediation actions: a review. Environments 9 (1), 11.
Needleman, H., 2004. Lead poisoning. Annu. Rev. Med. 55 (1), 209–222.
Nikoonahad, A., Naserifar, R., Alipour, V., Poursafar, A., Miri, M., Ghafari, H.R., et al., 2017. Assessment of hospitalization and mortality from exposure to PM10 using AirQ modeling in Ilam, Iran. Environ. Sci. Pollut. Res. 24 (27), 21791–21796.
Pant, P., Harrison, R.M., 2012. Critical review of receptor modelling for particulate matter: a case study of India. Atmos. Environ. 49, 1–12.
Pant, P., Shi, Z., Pope, F.D., Harrison, R.M., 2017. Characterization of traffic-related particulate matter emissions in a road tunnel in Birmingham, UK: trace metals and organic molecular markers. Aerosol Air Qual. Res. 17 (1), 117–130.
Rečnik, A., Zavašnik, J., Fajmut-Štrucl, S., 2014. The Mežica mine, Koroška (Slovenia). Mineral. Rec. 45 (5), 507–548.
Rogan Šmuc, N., Žerdoner, T., Zuliani, T., et al., 2025. Personal Communication not published.
Sen, I.S., Bizimis, M., Tripathi, S.N., Paul, D., 2016. Lead isotopic fingerprinting of aerosols to characterize the sources of atmospheric lead in an industrial city of India. Atmos. Environ. 129, 27–33.
Shiel, A.E., Weis, D., Orians, K.J., 2010. Evaluation of zinc, cadmium and lead isotope fractionation during smelting and refining. Sci. Total Environ. 408 (11), 2357–2368.
Snoj Tratnik, J., Falnoga, I., Mazej, D., Kocman, D., Fajon, V., Jagodic, M., et al., 2019. Results of the first national human biomonitoring in Slovenia: trace elements in men and lactating women, predictors of exposure and reference values. Int. J. Hyg Environ. Health 222 (3), 563–582.
Souto-Oliveira, C.E., Babinski, M., Araújo, D.F., Andrade, M.F., 2018. Multi-isotopic fingerprints (Pb, Zn, Cu) applied for urban aerosol source apportionment and discrimination. Sci. Total Environ. 626, 1350–1366.
Svete, P., Milačič, R., Pihlar, B., 2001. Partitioning of Zn, Pb and Cd in river sediments from a lead and zinc mining area using the BCR three-step sequential extraction procedure. J. Environ. Monit. 3 (6), 586–590.
Vecchi, R., Marcazzan, G., Valli, G., 2007. A study on nighttime–daytime PM10 concentration and elemental composition in relation to atmospheric dispersion in the urban area of Milan (Italy). Atmos. Environ. 41 (10), 2136–2144.
Wagner, S., Santner, J., Irrgeher, J., Puschenreiter, M., Happel, S., Prohaska, T., 2022. Selective diffusive gradients in thin films (DGT) for the simultaneous assessment of labile Sr and Pb concentrations and isotope ratios in soils. Anal. Chem. 94 (16), 6338–6346.
Wang, L., Jin, Y., Weiss, D.J., Schleicher, N.J., Wilcke, W., Wu, L., et al., 2021. Possible application of stable isotope compositions for the identification of metal sources in soil. J. Hazard Mater. 407, 124812.
Wedepohl, K.H., 1995. The composition of the continental crust. Geochem. Cosmochim. Acta 59 (7), 1217–1232.
WHO global air quality guidelines, 2021. Particulate Matter (PM2.5 and PM10), Ozone, Nitrogen Dioxide, Sulfur Dioxide and Carbon Monoxide. World Health Organization.
Yang, L., Tong, S., Zhou, L., Hu, Z., Mester, Z., Meija, J., 2018. A critical review on isotopic fractionation correction methods for accurate isotope amount ratio measurements by MC-ICP-MS. J. Anal. At. Spectrom. 33 (11), 1849–1861.
Yoshinaga, J., Yamasaki, K., Yonemura, A., Ishibashi, Y., Kaido, T., Mizuno, K., et al., 2014. Lead and other elements in house dust of Japanese residences – source of lead and health risks due to metal exposure. Environ. Pollut. 189, 223–228.
Zhang, K., Chai, F., Zheng, Z., Yang, Q., Zhong, X., Fomba, K.W., et al., 2018. Size distribution and source of heavy metals in particulate matter on the lead and zinc smelting affected area. J. Environ. Sci. 71, 188–196.
Žibret, G., Gosar, M., Miler, M., Alijagić, J., 2018. Impacts of mining and smelting activities on environment and landscape degradation—Slovenian case studies. Land Degrad. Dev. 29 (12), 4457–4470.
Zuliani, T., Mladenovič, A., Ščančar, J., Milačič, R., 2016. Chemical characterisation of dredged sediments in relation to their potential use in civil engineering. Environ. Monit. Assess. 188 (4), 234.